



## Gas-phase ion migration spectrum analysis of the volatile flavors of large yellow croaker oil after different storage periods

Tengfei Zhao<sup>a</sup>, Zhongqi Cao<sup>b</sup>, Jin Yu<sup>c</sup>, Xudong Weng<sup>c</sup>, Soottawat Benjakul<sup>d</sup>,  
Alessandra Guidi<sup>e</sup>, Xiaoguo Ying<sup>a,c,\*\*</sup>, Lukai Ma<sup>f,g,\*</sup>, Gengsheng Xiao<sup>f</sup>, Shanggui Deng<sup>a</sup>

<sup>a</sup> Zhejiang Provincial Key Laboratory of Health Risk Factors for Seafood, Collaborative Innovation Center of Seafood Deep Processing, College of Food and Pharmacy, Zhejiang Ocean University, Zhoushan, 316022, China

<sup>b</sup> Sinopec Dalian Research Institute of Petroleum and Petrochemicals, Dalian Liaoning, 116045, China

<sup>c</sup> Longyou Aquaculture Development Center, Agricultural and Rural Bureau of Longyou County, Quzhou, 324000, China

<sup>d</sup> International Center of Excellence in Seafood Science and Innovation, Faculty of Agro-Industry, Prince of Songkla University, Hat Yai, Songkhla, 90110, Thailand

<sup>e</sup> Department of Agriculture, Food and Environment (DAFE), Pisa University, Via Del Borghetto, 80, 56124, Pisa, Italy

<sup>f</sup> Guangdong Provincial Key Laboratory of Lingnan Specialty Food Science and Technology, College of Light Industry and Food, Zhongkai University of Agriculture and Engineering, Guangzhou, 510225, China

<sup>g</sup> Academy of Contemporary Agricultural Engineering Innovations, Zhongkai University of Agriculture and Engineering, Guangzhou, 510225, China

### ARTICLE INFO

Handling editor: Alejandro G. Marangoni

#### Keywords:

Large yellow croaker (*Larimichthys crocea*)  
Fish oil  
Electronic nose  
Fingerprint  
Flavor substance

### ABSTRACT

The large yellow croaker, a species of fish found in the northwestern Pacific, is favored by consumers because of its prevalence in saltwater bodies, golden yellow abdomen, high calcium content, high protein, high fat content, and a flavor that originates from its lipids and volatile components. Volatile organic compounds significantly affect the aroma of food. In this work, electronic nose and headspace gas chromatography-ion mobility spectrometry were applied to analyze the flavor differences in fish oil durations. Through electronic nose system analysis, sensors W1C, W3S, W6S, and W2S directly affected fish oil flavor, and their flavor components were different. Gas chromatography-ion mobility spectrometry identified 26 volatile components (19 aldehydes, 3 ketones, 2 alcohols, 1 furan, and 1 olefin). (*E,E*)-2,4-hexadienal (D), (*E,E*)-2,4-hexadienal (M), 2,4-heptadienal (M), (*E*)-2-octenal, 2-propanone, 2-heptanone (M), 3-pentanone (D), and 1-octen-3-ol were the key flavor components of the fish oil. In conclusion, the combination of GC-IMS and PCA can identify the differences in flavor changes of large yellow croaker oil during 0–120 days storage. After 60 days storage, the types and signals of 2-propanone, 2-heptanone (M) components increase significantly. When 120 days storage, at this time, (*E,E*)-2,4-hexadienal (D), (*E,E*)-2,4-hexadienal (M), 2,4-heptadienal (M), (*E*)-2-octenal, (*E*)-2-octenal significantly. It has become the main flavor substance of fish oil. In summary, as the storage period increases, the components increase, and the oxidizing substances will increase, resulting in the deterioration of fish oil.

### 1. Introduction

In recent years, the use of science to create health products with high nutritional value has become increasingly popular. Fish oil from large yellow croakers is a high-quality natural oil, containing essential fatty acids, unsaturated fatty acids, and various active components, which is also easy to digest and absorb (Donovan et al., 2020; Du et al., 2022; Navarro et al., 2020). However, the quality of this fish oil merits further study because the large yellow croaker undergoes lipid oxidation during storage, leading to the contamination and quality deterioration of its oil

(Cao et al., 2021). With changing human dietary habits, identifying the health benefits and high-nutrition components of food has acquired significant importance (Jadwiga et al., 2019). Fish oil has beneficial effects on the human body; for instance, it regulates blood lipids, promotes brain development, improves vision, and prevents cardiovascular and cerebrovascular diseases and senile dementia (L. Li et al., 2020; IlesanmiOyelere et al., 2020; Lysfjord et al., 2021; Galindo et al., 2021). The changes in the nutrients of fish oil are affected by the oxidation rate and time, temperature, and light irradiation from the environment (Ade et al., 2014). During oxidation, fish oil generates adverse components such as small-molecular aldehydes, ketones, alcohols, and acids (Chen

\* Corresponding author. No.24 Dongsha Road, Haizhu District, Guangzhou, Guangdong province, 510225, PR China.

\*\* Corresponding author. No.1 Haida South Road, Linceng Changzhi Island, Zhoushan, Zhejiang province, 316022, PR China.

E-mail addresses: [yingxiaoguo@zjou.edu.cn](mailto:yingxiaoguo@zjou.edu.cn) (X. Ying), [malukai@zhku.edu.cn](mailto:malukai@zhku.edu.cn) (L. Ma).

<https://doi.org/10.1016/j.crfs.2022.04.012>

Received 5 March 2022; Received in revised form 11 April 2022; Accepted 28 April 2022

Available online 8 May 2022

2665-9271/© 2022 The Authors. Published by Elsevier B.V. This is an open access article under the CC BY-NC-ND license (<http://creativecommons.org/licenses/by-nc-nd/4.0/>).

### Abbreviations

AV	acid value
CDV	conjugated diene value
GC	gas chromatography
HS	headspace
IMS	ion mobility spectrometry
MS	mass spectrometry
<i>p</i> -AV	<i>p</i> -anisidine value
POV	peroxidation value
PCA	principal component analysis
RIP	reaction ion peak
SPME	solid-phase microextraction

et al., 2018).

Recently, a novel flavor identification technique named gas chromatography-ion mobility spectrometry (GC-IMS) has gained rising popularity in food flavor detection (Sullivan and Budge, 2012; Wang et al., 2020). It combines the high separation capability of GC with IMS to establish a fingerprint of volatile components, classify their adulteration degree, and evaluate the freshness of food through odor testing (Yang et al., 2021; X.X. Li et al., 2020; Tian et al., 2020; Mutlu et al., 2021).

In a previous study, the volatile components of crab meat were characterized by solid-phase microextraction (SPME) and GC tandem spectroscopy, revealing that the relative contents of 3-methylbutyraldehyde, heptanaldehyde, and benzaldehyde contributed to improving the flavor (Deng et al., 2021). Encina et al. studied the changes in the odor and fatty acid content of tuna oil and squid oil (Encina et al., 2018). The volatile flavor content was analyzed by GC-IMS, and the results showed that the flavors of 2,4-heptadienyl and 2-valeric aldehyde were most significant. It has further been reported that changes in the volatile compounds in fish oil purification can be detected by headspace (HS) and SPME with GC-MS (Song et al., 2018). Despite this, the effects of different storage periods on large yellow croaker oil have not been analyzed by GC-IMS, and the identification of its volatile flavors are rarely reported. Therefore, conducting such research has the potential to greatly keep the flavor of fish oil and expand its application in the food industry.

In our previous research, we reported the use of GC-IMS and principal component analysis (PCA) to identify differences in the flavor components of large yellow croaker meat during storage (Zhao et al., 2021a,b). We found that 3-methylbutanol (trimer), 3-methylbutanol (D), 3-pentanone (D), and 3-pentanone (M) contents increased (where D and M indicate dimer and monomer, respectively) and were the key components affecting the fish meat flavor. Based on these results, we continued experimenting on large yellow croaker oil and found that the storage period of the oil is also particularly important to its flavor, and that the sensory characteristics of fish oil are closely related to its characteristic flavor substances (Zhao et al., 2021a,b). In addition, the sensory characteristics of fish oil can not only reflect its overall quality, but also characterize the oxidation degree of oil itself. It has been reported that the main reason for the deterioration of fish oil flavor is the volatile compounds of the oil, (*E,E*)-2,4-hexadienal (D) and 2,4-heptadienal (M) (Kazuo et al., 2018).

Comprehensive above, GC-IMS was used to detect the volatile flavor substances produced in the oxidation of fish oil over storage period, and determine its volatile flavor fingerprint during oxidation. The data gathered here provide valuable insights into in the volatile flavor compounds of fish oil, the oxidation mechanisms, and its safe consumption by humans.

## 2. Materials and methods

### 2.1. Fish samples

The yellow croaker variety selected in this study was the large yellow croaker from Zhoushan (Zhejiang). According to previous studies (Zhao et al., 2021a,b), the nutritional indexes of large yellow croaker were as follows. The fish was stored at  $-18^{\circ}\text{C}$  (MDF-U53V, Sanyo, Japan) and a relative humidity of 60–75% for 0, 5, 10, 20, 30, 40, 60, 90, and 120 days. At specific times, the fish meat was cut and homogenized at 10000 rpm for 20 s (FJ200-S, Hunan Li Chen Instrument Technology Company, China), Extract oil through fat extractor. The subsequent experimental indexes were determined from fish oil. For the identification of volatile components of large yellow croaker oil during different storage periods, GC-IMS instrument was used to analyze the fish oil samples, which were determined during 0, 60, 90 and 120 days respectively.

component	content
Length	19.40–24.00 cm
Weight	270.50–320.70 g
salt-soluble protein	11.90 g/100 g
water-soluble protein	14.27 g/100 g
water content	61.85 g/100 g
Ash	0.80 g/100 g

### 2.2. Reagents

Ethanol, petroleum ether, trichloromethane, sodium sulfate, acetic acid, phenolphthalein indicator, isooctane, n-hexane, n-heptane, potassium iodide, phenol, potassium hydroxide, tetrahydrofuran, and alumina were purchased from Sinopharm Chemical Reagent Co., Ltd. (Shanghai, China).

### 2.3. Raw material processing

Material processing were prepared according to previous scientific research work (Zhao et al., 2021a,b). The fish oil was collected with a fat extractor (Soxtec FOSS, Fos Analysis Company, China). The detailed procedure is shown in Fig. 1.

### 2.4. Determination of oxidation index

The official methods prescribed by the American Oil Chemists Society (AOCS) were used to determine the AVs (Ca 5a-40), POVs (Cd 8b-90), and *p*-anisidine values (*p*-AVs; Cd 18–90) of the various samples. The conjugated diene value (CDV) was determined by modifying an existing approach (Ma et al., 2020).

#### 2.4.1. Acid values

For the phenolphthalein indicator, 1.00 g (Ar224-CN, Ohaus Instrument Co., Ltd., China) of phenolphthalein solid was dissolved in 95% ethanol, ultrasonicated until complete dissolution, and then transferred to a 100 mL capacity bottle. A standard solution of 0.01 mol/L potassium hydroxide was prepared using 0.56 g of potassium hydroxide dissolved in 1000 mL of deionized water. The fish samples (5.00 g) were added to a 50 mL mixture of petroleum ether and ethanol (2:1, v/v). Subsequently, 2–3 drops of the phenolphthalein indicator were added to the mixture, and the solution (micro-red) was titrated with a standardized solution of 0.01 mol/L sodium hydroxide. The AV of the sample was calculated according to Eq. (1):

$$AV = (V \times c \times 56.1)/m \quad (1)$$

where  $V$  is the volume of the potassium hydroxide solution (mL),  $c$  = 0.01 mol/L is the concentration of potassium hydroxide,  $m$  is the mass of the oil sample (g), and the number 56.1 indicates the molar mass (g/

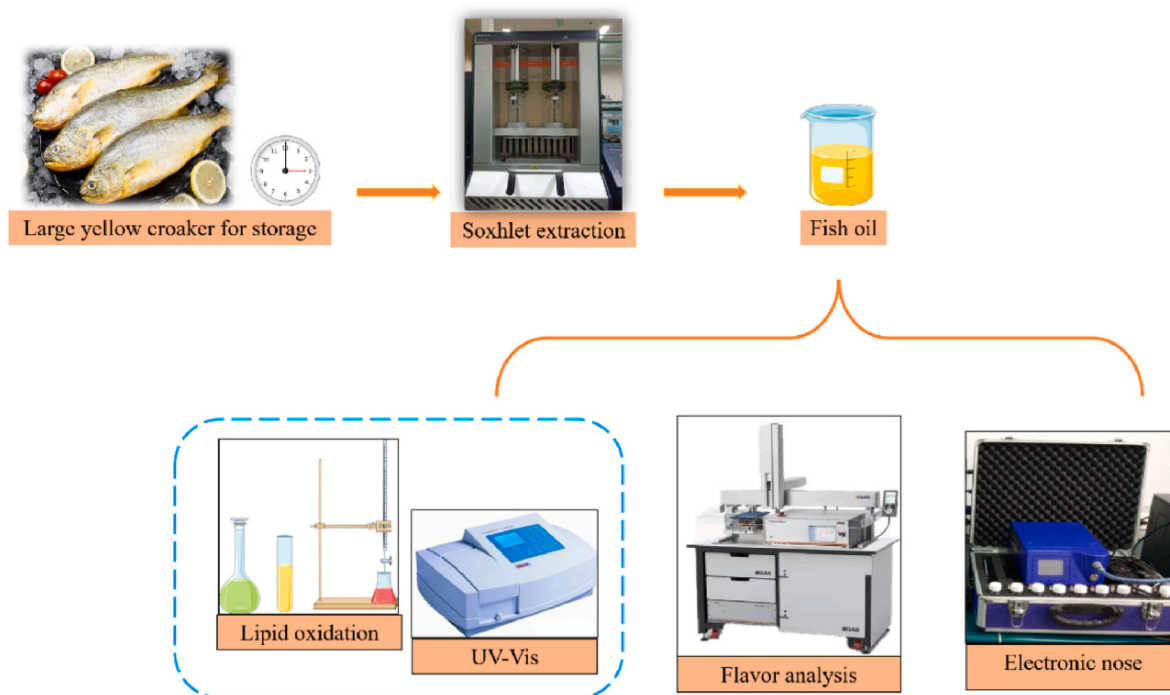


**Fig. 1.** Schematic illustrating the procedure to determine the components of large yellow croaker oil by physical and chemical methods. (For interpretation of the references to color in this figure legend, the reader is referred to the Web version of this article.)

mol) of potassium hydroxide.

#### 2.4.2. Peroxide values

To prepare a standard solution of sodium thiosulfate (Ma et al., 2021), 1.60 g of anhydrous  $\text{Na}_2\text{S}_2\text{O}_3$  solid was added to a small beaker with 0.02 g  $\text{Na}_2\text{CO}_3$ . The chemicals were then dissolved in 100 mL of water. The solution was diluted ten times to a concentration of 0.005 mol/L. Subsequently, 5.00 g of fish oil was added to a 250 mL conical bottle, after which 5 mL of an acetic acid-iso-octane solution (3:2, v/v) and 0.50 mL of saturated potassium iodide solution were added. After 1 min of mixing, 30 mL of deionized water was added to the aforementioned sodium sulfate standard solution, leading to blue coloration. Next, 0.50 mL of starch solution was added dropwise until the blue color disappeared at the end of titration. The POV (meq/kg) was calculated according to Eq. (2):

$$POV = (1000 \times V \times c) / m \quad (2)$$

where  $c$  is the concentration of the standardized thiosulfate solution (mol/L).

#### 2.4.3. *p*-Anisidine values

The *p*-anisidine solution was prepared by adding *p*-anisidine (0.125 g) to glacial acetic acid (50 mL). A sample (2.00 g) of the fish oil was then added to a 25 mL volumetric flask, and iso-octane (25 mL) was added prior to swirling to mix well. The absorbance ( $A_0$ ) of the resulting solution was measured at 350 nm using a spectrophotometer (UV-2600, Tianjin, China). An portion (5 mL) of the solution sample was then pipetted into a test tube, and the *p*-anisidine reagent (1 mL) was added. After 10 min, the sample absorbance ( $A_1$ ) was measured at 350 nm. For the blank sample, iso-octane (5 mL) and the *p*-anisidine reagent (1 mL) were added to a separate test tube. The dimensionless *p*-AV was calculated according to Eq. (3):

$$p-AV = 25(1.2A_1 - A_0) / m \quad (3)$$

where  $A_1$  is the absorbance of the fat solution after reaction with the *p*-anisidine reagent,  $A_0$  is the initial absorbance of the fat solution, the

number 25 indicates the sample volume (25 mL), and 1.2 is the correction factor.

#### 2.4.4. Conjugated diene values

The fish oil sample was weighed and placed in a small beaker. After the addition of iso-octane (5 mL) to dissolve the sample, the volume was adjusted to 50 mL using an additional volume of iso-octane. The optical absorption of the obtained solution was then measured at 232 nm (UV-2600, Yercu Instrument Co., Ltd., China) using iso-octane as the zero reference. The CDV was calculated according to Eq. (4):

$$CDV = Aq \times c \times 1 \quad (4)$$

where  $Aq$  is the absorbance of the sample at 232 nm,  $c$  is the mass concentration of the sample (g/100 mL), and 1 (cm) is the length of the quartz cell.

#### 2.5. Detection of volatile flavor substances

For sample pretreatment, the fish oil (2.00 g) was sealed in a capped bottle and allowed to stand for 30 min to allow the volatile compounds to equilibrate in the air. An electronic nose (PEN3, Airsense, Berlin, Germany) was employed under previously reported conditions ( $n = 3$ ) (Emre, 2021). The various sensors are described in Table S1.

#### 2.6. Construction of the fingerprint map of the flavor profiles

##### 2.6.1. Sample processing

After thawing at 4 °C in a refrigerator, 5.00 g of fish oil was weighed and placed in a 20 mL HS bottle equipped with a magnetic screw seal. The sampling test was conducted after incubation at 40 °C for 20 min. GC-IMS analysis was carried out in triplicate.

##### 2.6.2. GC-IMS conditions

Based on the data by Jia (Jia et al., 2021), the GC-IMS conditions in

the following table were slightly modified.

Condition	Specifications
Column type	MXT-5, 15METER, 0.53 mmID, 1.0UMDF
Column temperature	60 °C
Chromatographic analysis time	25 min
Carrier gas/drifting gas	N <sub>2</sub> (purity >99.99%)
IMS temperature	45 °C
Automatic top injection volume	500 µL
Headspace incubation	40 °C, 20 min
Headspace injection needle temperature	85 °C
Injection volume	1 mL
Incubation speed	5000 r/min

### 2.6.3. Detection method

The gas sample in the HS bottle was extracted using a heated injection needle. The volatile components in the gas sample were identified using a flavor analyzer (FlavourSpec®, G.A.S. Company, Germany).

### 2.7. Data processing

Origin software (OriginLab Corporation, Northampton, Massachusetts, USA) was used to process the data. The means and standard deviations were determined by SPSS 24.0 software (Chicago, IL, USA), and a multi-comparison was outputted ( $p < 0.05$ ). The volatile substances were tested with Vocal analysis software and equipment. NIST IMS databases and the dynamic PCA plug-in program were used to perform dynamic master component analysis.

## 3. Results and discussion

### 3.1. Lipid oxidation properties

Four indicators (AV, POV, *p*-AV, and CDV) were used to assess oxidation in the oil from the large yellow croaker during storage. Fig. 2 shows that all four values increase significantly during storage ( $p < 0.05$ ). In the fresh fish oil (0 d), the AV, POV, *p*-AV, and CDV were  $0.58 \pm 0.13$  mg/g,  $10.98 \pm 0.56$  meq/kg,  $0.31 \pm 0.05$ , and  $22.24 \pm 0.21$ , respectively. These values meet the national standard (GB 5009.229–2016), indicating that the fresh fish oil was highly nutritious (Tu et al., 2021).

After 90 d, these values increased to  $2.75 \pm 0.10$  mg/g,  $41.04 \pm 0.76$  meq/kg,  $1.34 \pm 0.06$ , and  $31.76 \pm 0.25$ , respectively. In particular, the POV increased by approximately four times during storage, possibly because hydrogen peroxide is the main product of fish oxidation (Elavarasan and Shamasundar, 2021). With an increase in the storage period, fat oxidation in the fish oil led to an increase in the POV. Temperature changes can also cause the isomerization and decomposition of triglyceride and other substances. Additionally, the four-fold increase in the POV during storage is likely assisted by the development of hydroperoxide, the primary product of lipid oxidation (Thimmappa et al., 2019), which further decomposes into low-molecular-weight ketones, aldehydes, and other secondary oxidation products.

At 120 d, the AV, POV, *p*-AV, and CDV were  $3.77 \pm 0.14$  mg/g,  $75.16 \pm 0.85$  meq/kg,  $1.94 \pm 0.07$ , and  $43.29 \pm 0.23$ , respectively. The increased AV is closely related to the free fatty acid content (Malik et al., 2021). It has been reported that the oxidation of fish oil during storage causes the breakage of ester bonds, releasing a large amount of free fatty acids that increase the AV (Crexi et al., 2009; Zhang et al., 2021). The

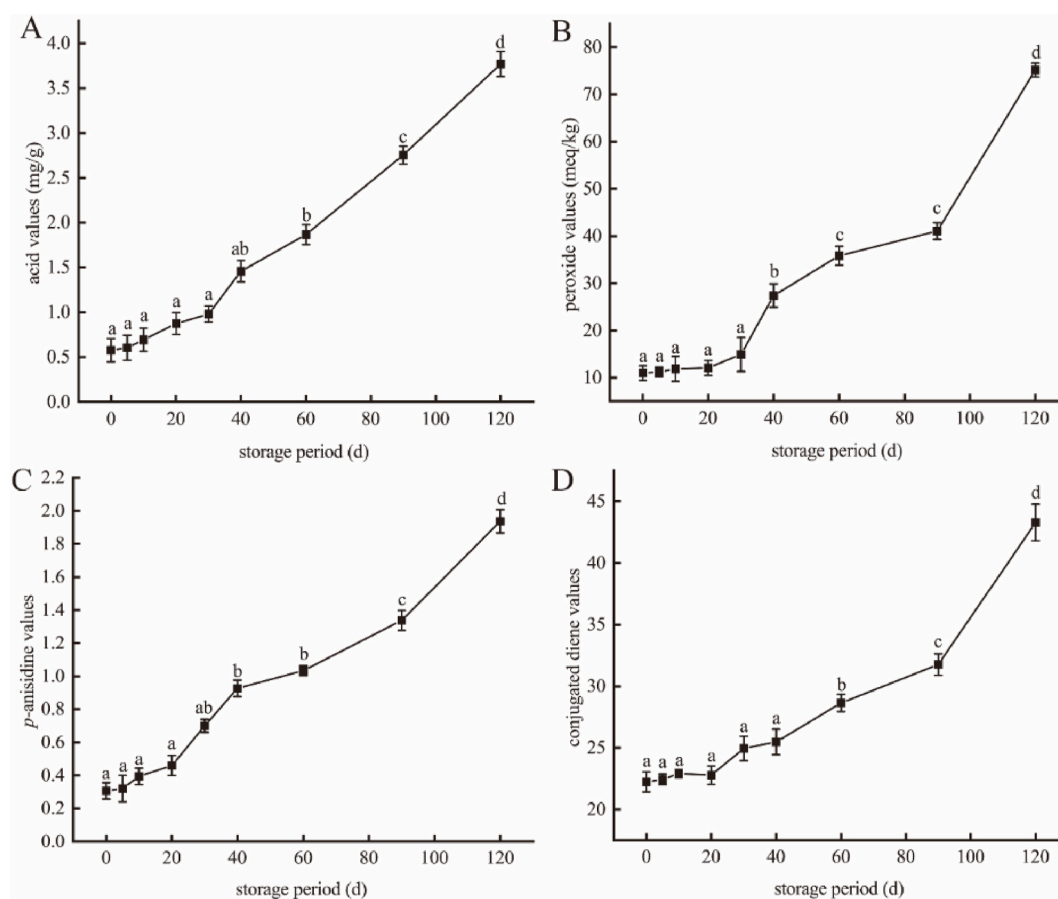


**Fig. 2.** Lipid oxidation properties of large yellow croaker oil at different storage periods. A: acid values; B: peroxide values; C: *p*-anisidine values; D: conjugated diene values. *p*-anisidine values and conjugated diene values have no units. Data points are plotted as means  $\pm$  SD ( $n = 3$ ).

*p*-AV obtained from the quantitative characterization of the secondary oxidation product indicated the presence of aldehyde compounds in the oil. The *p*-AV and POV were similar, which is associated with an increased content of oxidation products in the fish.

### 3.2. Volatile component identification

To illustrate changes in the volatile flavor compounds during storage, we measured their contents at 0, 60, 90, and 120 d and visualized the results, respectively. The samples were analyzed based on the retention and drift times of the column of the ion migration system (Jia et al., 2021). The qualitative analysis results for the volatile components of the large yellow croaker oil are shown in Fig. 3. The retention and drift times of the ion migration spectra presented in Fig. 3 are summarized in Table 1. A total of 26 peaks, corresponding to 5 component groups, were identified. These include 19 aldehydes, 3 ketones, 2 alcohols, 1 furan, and 1 olefin. When passing through the drift zone, a single compound can be observed as it forms a complex between the analyzed ions and neutral molecules (dimers and trimers).

Fig. 4 plots the signal strengths measured by the electronic nose with different sensors for the fish oil samples. With prolonged storage, the signals from the W3C, W6S, W2W, W3S, and W1C sensors became stronger, indicating that the large yellow croaker oil accumulates aromatic and hydrogen peroxide; however, the signals for the organic sulfide compounds decreased from 0 to 90 d and then rebounded at 120 d. This resembles the formation and flavor changes for heterocyclic aromatics reported by Meng (Li et al., 2022). Aromatics, alkanes and aliphatics, hydrides, sulfides, ethanol, and some aromatics were determined by the W1C, W3S, W6S, W1W, W2S, and W6S sensors, respectively. The threshold of alkanes is high, so they barely contribute to the odor. The W3C and W2W sensors provided a small response value, highlighting the low concentrations of ammonia and aromatic compounds in the large yellow croaker oil. This experimental result agrees with theoretical expectations (Salsinha et al., 2021).

### 3.3. Analysis of topographic differences

GC-IMS was employed to output a three-dimensional (3D) terrain visualization to explore the influence of the storage period on the volatile compounds (Cui et al., 2020). The overall pattern is similar among the different storage periods, but there are minor visible variations in the signal intensity. The GC-IMS data are visualized as a 3D terrain in Fig. 5 to easily observe and compare the compositions of the volatile substances. Overall, the content of volatile compounds was the highest in

fresh fish oil (0 d), and continuously declined with storage up to 120 d.

In Fig. 6 the red vertical line indicates the reaction ion peak (RIP), and each point on the right side of the RIP represents different volatile compounds in the sample. The signal is substantial within the retention time of 100–300 s and drift time of 1.0–2.0 s. In the normalized two-dimensional (2D) plots, the red (blue) color indicates an increase (decrease) in the volatile compound concentration compared to the reference (Duan et al., 2021a,b). It has been suggested that the drift rate is related to the concentration of fish samples (B. Zhang et al., 2020). The 2D topographic map for fresh (0 d) fish oil samples was selected as a reference. The other three spectra obtained after storage were derived from the reference. If the amount of the volatile compound does not vary over time, the color is white. The red color indicates that the volatile compound concentration is higher than that of the reference. The blue color indicates that the volatile compound concentration is lower than that of the reference. The figure shows that the signal strength of the compound is higher in the 120 d fish oil, and that some compounds have a slightly lower concentration after 60 d and 90 d of storage.

### 3.4. Volatile flavor compounds

To further compare the volatile flavor compounds in the samples after different storage periods, the GC-IMS 2D map was used to identify the peaks, as shown in Fig. 7. In the fingerprint, the brighter the color, the higher the content (Yao et al., 2020). Different concentrations of a single compound will produce various signals and spots. The fingerprint shows many unknown substances (X. Chen et al., 2021; Yu et al., 2021). In Fig. 7, the area and brightness of coloration for the volatile organic compounds represent the concentration of the substances. White indicates low density, red indicates high density, and the darker the color, the higher the density. A total of 26 compounds were identified, including 19 aldehydes, 3 ketones, 2 alcohols, 1 furan, and 1 olefin. The content of substances numbered 6, 9, 10, 11, 12, 13, 14, and 18 gradually increased with increasing storage period, while that of compound 15 decreased. The concentration of compounds 16 and 17 was the highest during 90 d, showing a trend of first increasing and then decreasing. The large yellow croaker oil sample contained many aldehydes. This result is similar to that of Duan (Duan et al., 2021a,b), who used GC-IMS to determine the flavor of meat products, which is mainly reflected in a higher aldehyde content.

Aldehydes are the main flavor components of large yellow croaker oil. Most aldehydes have a low flavor threshold and a characteristic fatty aroma at a low concentration. However, when the concentration is higher than a certain critical value, they will produce putrefied, rancid,

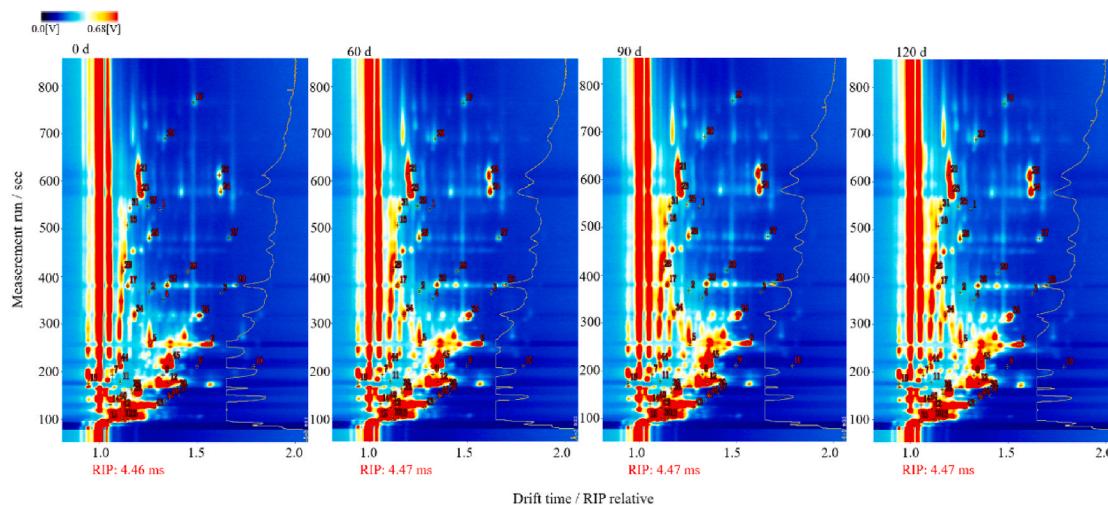
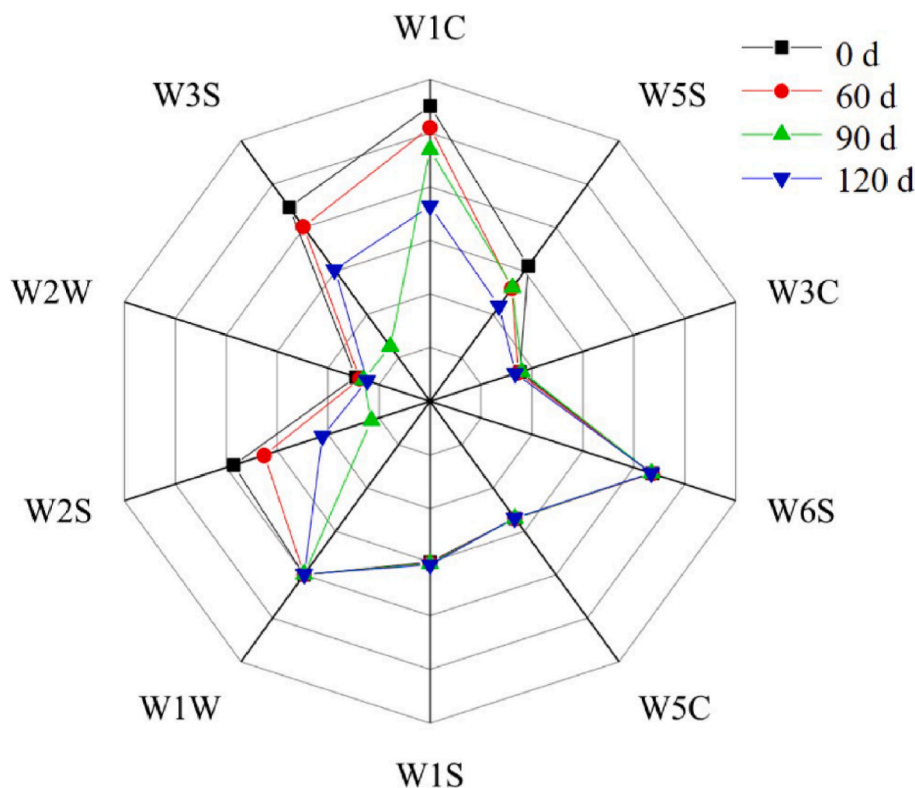


Fig. 3. Ion migration spectra of large yellow croaker oil at different stage periods. The x-axes represent the ion migration times and the y-axes represent the gas chromatographic retention times. (For interpretation of the references to color in this figure legend, the reader is referred to the Web version of this article.)

**Table 1**  
Qualitative analysis of flavor compounds in large yellow croaker oil after different storage periods.

No	Compound	CAS#	Molecular formula	MW	RI1	RT2	DT3	Storage periods			
								0 d	60 d	90 d	120 d
1	2-heptanone (M)	C110430	C7H14O	114.2	892	367.609	1.25645	82.87	95.35	108.29	95.04
2	3-pentanone (D)	C96220	C5H10O	86.1	694.1	176.751	1.35138	273.88	313.93	357.20	406.63
3	2-propanone	C67641	C3H6O	58.1	505.1	100.756	1.11999	126.91	139.03	145.79	139.21
4	hexanal (M)	C66251	C6H12O	100.2	793	257.755	1.26394	907.11	872.24	743.39	696.90
5	hexanal (D)	C66251	C6H12O	100.2	792.5	257.283	1.55986	505.45	481.12	390.43	355.89
6	n-nonanal	C124196	C9H18O	142.2	1102.9	765.255	1.48078	306.25	376.15	411.86	474.17
7	(E)-2-octenal	C2548870	C8H14O	126.2	1069.4	689.37	1.33717	496.00	591.03	715.58	835.52
8	(E,E)-2,4-heptadienal (M)	C4313035	C7H10O	110.2	1032.9	615.291	1.19819	344.01	401.55	436.32	461.33
9	(E,E)-2,4-heptadienal (D)	C4313035	C7H10O	110.2	1031.3	612.28	1.61359	142.82	188.13	254.66	290.86
10	2,4-heptadienal (M)	C5910850	C7H10O	110.2	1010.4	573.735	1.209	236.17	285.46	308.83	337.72
11	2,4-heptadienal (D)	C5910850	C7H10O	110.2	1012.4	577.348	1.62131	1073.04	1731.68	2175.73	2285.53
12	(E)-2-heptenal (M)	C1882955	C7H12O	112.2	961.2	479.634	1.25746	942.12	1082.78	1126.92	1135.88
13	(E)-2-heptenal (D)	C1882955	C7H12O	112.2	961.7	480.593	1.66231	197.97	349.82	434.62	527.71
14	(E,E)-2,4-hexadienal (M)	C142836	C6H8O	96.1	921.2	411.328	1.11926	901.61	937.22	1033.37	989.36
15	(E,E)-2,4-hexadienal (D)	C142836	C6H8O	96.1	920	409.362	1.45288	85.00	118.83	129.01	118.23
16	2-hexenal (M)	C505577	C6H10O	98.1	853.6	320.394	1.17916	545.85	618.71	743.53	874.97
17	2-hexenal (D)	C505577	C6H10O	98.1	851.5	317.942	1.51579	945.76	1339.46	1595.95	1683.76
18	ethanol	C64175	C2H6O	46.1	491.5	96.788	1.04578	181.97	194.69	201.30	212.76
19	1-penten-3-ol	C616251	C5H10O	86.1	690.1	174.053	0.94377	305.75	353.03	394.79	435.11
20	1-octen-3-ol	C3391864	C8H16O	128.2	993.7	543.635	1.15615	341.23	473.90	492.55	518.15
21	(E)-2-pentenal (M)	C1576870	C5H8O	84.1	747.8	217.199	1.10371	1601.99	1796.63	1868.25	1934.58
22	(E)-2-pentenal (D)	C1576870	C5H8O	84.1	753.5	222.004	1.36517	1236.68	1499.70	1578.89	1659.66
23	(Z)-4-heptenal	C6728310	C7H12O	112.2	900.6	380.069	1.1455	502.57	552.92	602.71	654.58
24	heptanal (M)	C111717	C7H14O	114.2	902.5	382.737	1.34747	773.41	784.55	791.95	836.28
25	heptanal (D)	C111717	C7H14O	114.2	902	382.036	1.69984	293.97	324.07	360.38	375.40
26	2-pentylfuran	C3777693	C9H14O	138.2	995.7	547.711	1.24728	187.62	201.00	219.79	230.96

**Note:** The retention times and ion migration times are listed together with the compound name, CAS number, molecular formula, molecular weight (MW), reserved index (RI1), retention time (RT2), drift time (DT3), and response peaks after different storage periods.



**Fig. 4.** Detection of volatile flavors from fish oil at different storage periods. 0 d, 60 d, 90 d, and 120 d represent the radar value of fish oil extracted from large yellow croaker meat in the corresponding storage periods. **Note:** W1C: Aromatics; W5S: Nitrogen oxides; W3C: Ammonia and aromatic components; W6S: Hydride; W5C: Olefins and aromatic molecules; W1S: Methane; W1W: Sulfides; W2S: Ethanol and some aromatics; W2W: Organic sulfides; W3S: Alkanes and aliphatics. (For interpretation of the references to color in this figure legend, the reader is referred to the Web version of this article.)

or other similar peculiar odors (Ana et al., 2020). The figure shows that the concentrations of the aldehyde compounds (*E,E*)-2,4-heptadienal (M) and 2,4-heptadienal (M) gradually increase. The concentrations of (*E*)-2-heptenal (M), 2-hexenal (M), and (*E*)-2-pentenal (M) gradually decrease from their highest values in the fresh stage, and those of

n-nonanal and heptanal (D) are the highest at 90 d, which may be caused by the gradual reduction in the n-nonanal carbon bonds contained in fish oil at 90 d (De et al., 2017). Among the ketones, the concentrations of 2-propanone, 2-heptanone (M), and 3-pentanone (D) gradually increase, which may be due to microbial degradation and lipid oxidation (Valdés

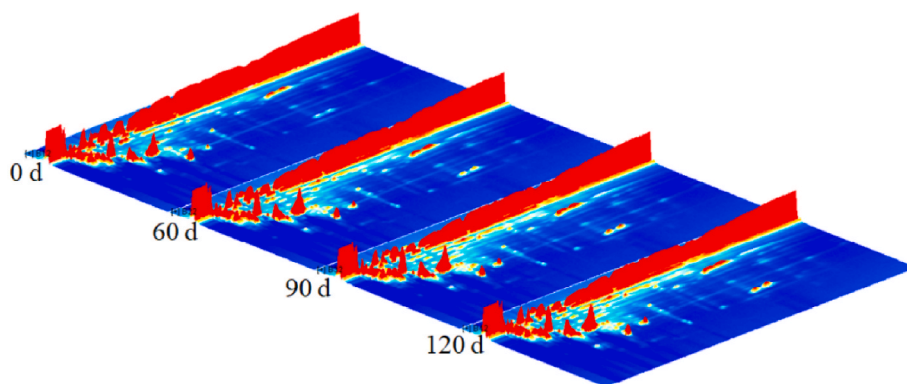


Fig. 5. 3D topographic map of large yellow croaker oil at different storage periods.

(x-axis: ion migration time, y-axis: GC retention time, and z-axis: peak height from quantification). (For interpretation of the references to color in this figure legend, the reader is referred to the Web version of this article.)

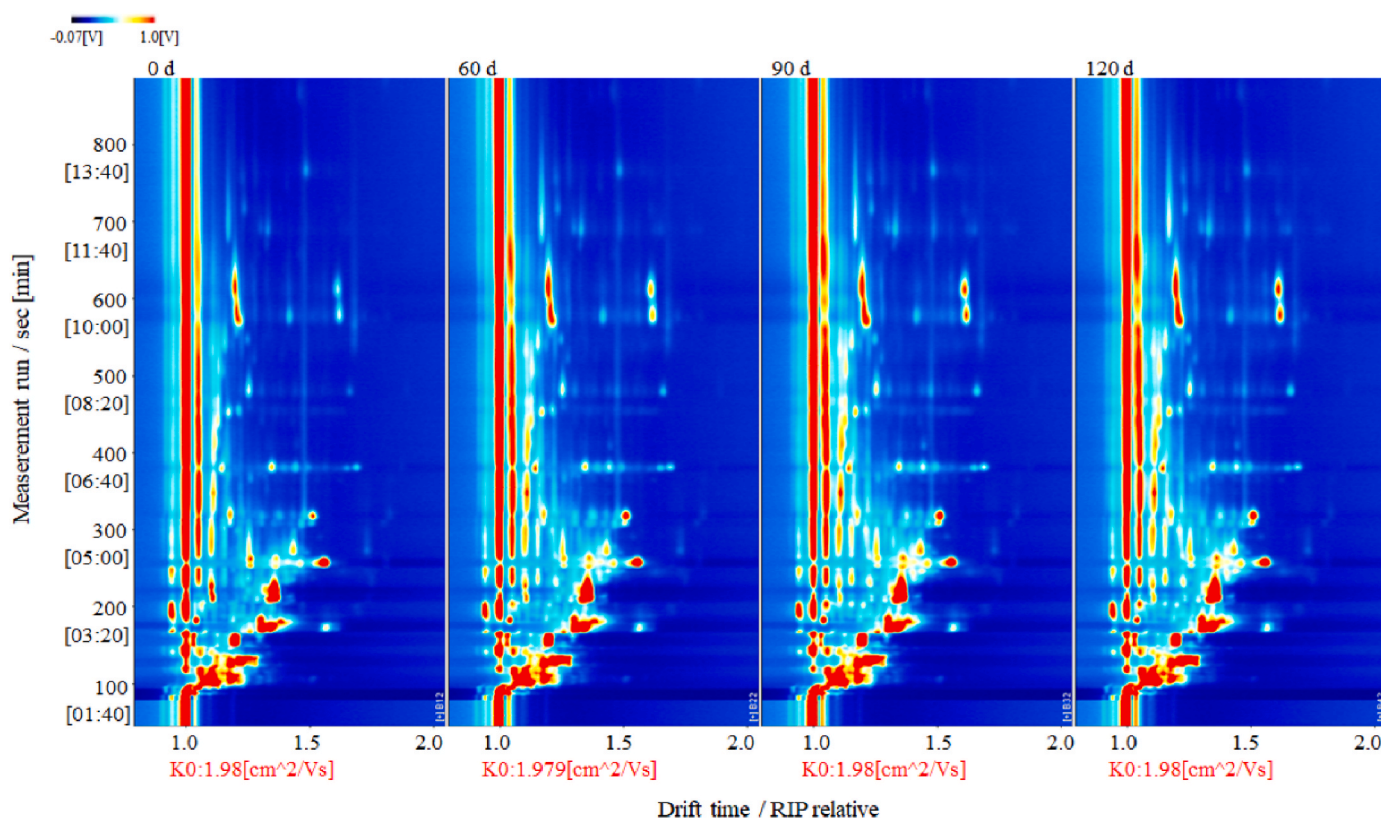
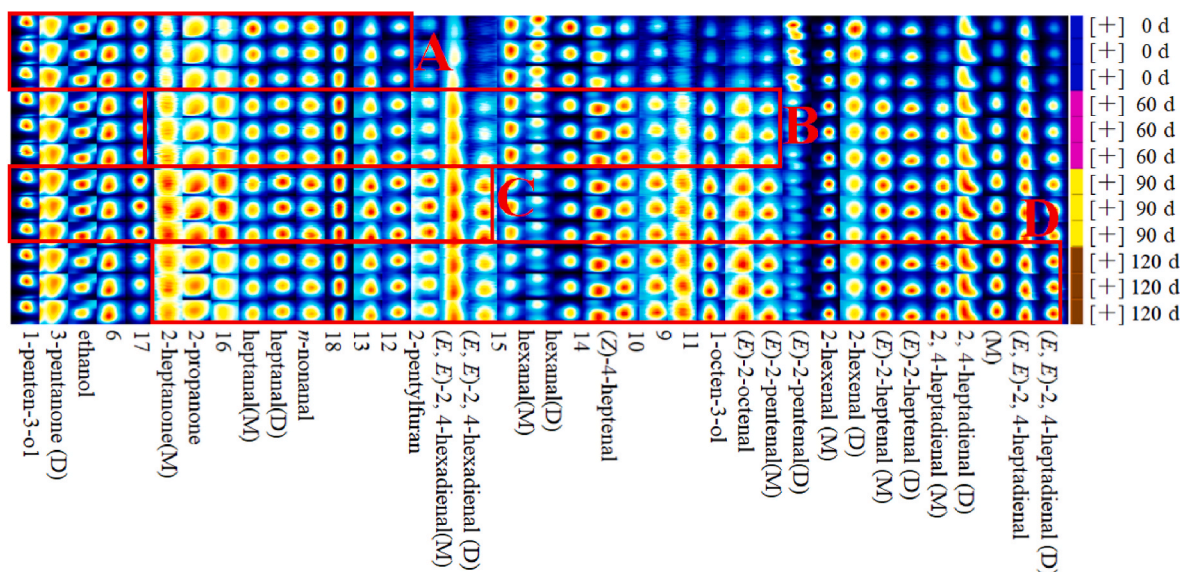


Fig. 6. Two-dimensional topographic map of fish oil at different storage periods.

et al., 2018). The oxidative precipitation of proteins and a reduction in oxidation will vary the flavor induced by the ketones (Y.P. Chen et al., 2021). The content of 1-octene-3-alcohol is very high, because fish oil will be affected by temperature, humidity and light after long-term storage, resulting in rotten taste. These rotten flavors are similar to pickles and spicy rotten eggs, which will accelerate the formation of bad flavor in large yellow croaker oil. The alcohol concentration is low during 0–90 d of storage, possibly because the quality is maintained and the extent of contamination is less (Granato et al., 2018). In addition, the content of 1-octen-3-ol in alcohols gradually increased and that of ethanol gradually decreased. As described previously, short-chain aldehyde flavor compounds are more likely to interact with protein aggregates to produce a fatty flavor (Dou et al., 2021). After a period of storage, when the n-nonanal content decreases and the fat content is

lowered, putrefied, rancid, or other peculiar odors are easily generated by these aldehyde volatile compounds, possibly due to the microbial degradation of free cysteine and methionine in fish muscle (Chie et al., 2021).

Ketone compounds are the second volatile flavor compounds, and many ketones can be generated by lipid oxidation or microbial degradation (Chen et al., 2017). Therefore, the main flavor changes in fish oil were mainly attributed to (*E,E*)-2,4-heptadienal (D), (*E,E*)-2,4-heptadienal (M), 2,4-heptadienal (M), (*E*)-2-pentenal(D), (*E*)-2-octenal, 1-octen-3-ol, (*Z*)-4-heptenal, (*E,E*)-2,4-hexadienal(M), 2-pentylfuran, 2-propanone, 2-heptanone(M), 3-pentanone (D), and 1-penten-3-ol.



**Fig. 7.** Characteristic fingerprint of large yellow croaker oil at different storage periods. **Note:** A–D represent sample storage periods of 0, 60, 90 and 120 d, respectively. The line represents the signal peak of one fish oil sample compound, and the column represents the signal peak of the volatile organic compounds in all different fish oil samples. The coloration is indicative of the content of the volatile compounds. (For interpretation of the references to color in this figure legend, the reader is referred to the Web version of this article.)

### 3.5. PCA of the flavor substances

During storage and transportation, large yellow croaker oil is vulnerable to external factors such as temperature, humidity, light and oxygen. Unsaturated fatty acids are easy to be oxidized. Finally, based on a detailed analysis of the GC-IMS and GC-MS results, we performed PCA using the fingerprint map of the volatile organic compounds (Fig. 8). This analytical method generates principal components that are linear combinations of the input variables, and is effective for reducing the number of variables and removing abnormal data (Zhou et al., 2021; Li et al., 2021). The resulting PCA model reflects the original state of the metabolic group data. The gathering of the sample can be determined from the PCA score map (Q. Zhang et al., 2020). Fig. 8 plots the PCA results for the fish oil samples after different storage periods. Overall, 80% of the data can be explained by the first principal component (PC-1) and 14% by the second principal component (PC-2). These contributions significantly change up to 60 d, and barely change for 90 and 120 d. The main difference between the 90 and 120 d samples arises from the fuel

sample distribution points. These results are similar to those obtained by Jia (Jia et al., 2020). It has also been reported that volatiles are produced in oil, especially esters and alcohols (Mi et al., 2021). Thus, fingerprint was successfully established using GC-IMS. The clustering of the triplicate data confirmed good reproducibility of the measurement.

### 4. Conclusion

To explore the changes in flavor of large yellow croaker fish oil during storage, HS-GC-IMS and PCA were used to determine. The main chemical determinations included AV, POV, *p*-AV, CDV, and the identification of various flavor substances. We identified 26 flavor substances in the fish oil samples and showed that the components of aldehydes, alcohols, and ketones were significantly different after different storage periods. (*E,E*)-2,4-hexadienal (M), 1-octen-3-ol, and 2-heptanone (M) were the main components contributing to the unpleasant flavor of the fish oil. In addition, the PCA results showed that the differences in the distributions of volatile compounds in the fresh

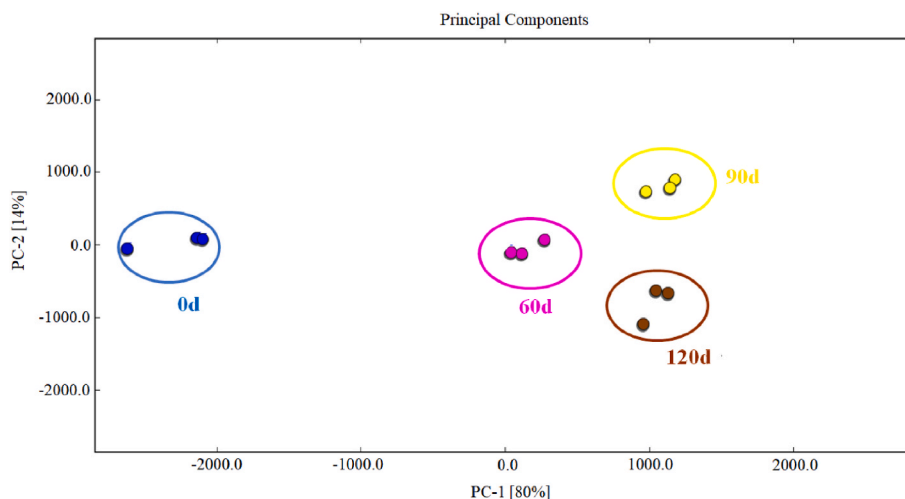


**Fig. 8.** PCA map of the characteristic flavors of large yellow croaker oil at different storage periods. (For interpretation of the references to color in this figure legend, the reader is referred to the Web version of this article.)

fish oil and the aged oil were relatively large and easy to distinguish; however, the differences in the distributions between 60, 90, and 120 d of storage were not as significant. Therefore, a specific and feasible method for constructing the flavor fingerprints of the given samples was established by HS-GC-IMS and PCA to successfully characterize the volatile flavor differences in fish oil. The combination of HS-GC-IMS and PCA made it possible to quickly detect and analyze the unique flavor fingerprint of fish oil. Additionally, the qualitative characteristics of fish during storage could be judged by scientific methods to maintain fish oil quality. The techniques employed herein could, therefore, be employed to improve quality control and inventory monitoring, as well as to analyze the flavor components present in other foodstuffs during storage. To ensure the continuous progress of this research, our team is still working in relation to this project, and we hope you look forward to our future report.

## Funding

This work was financed by the Scientific Research Business of Colleges and Universities in Zhejiang Province (Project No. 2021JZ010), Zhejiang Leading Training Program (2021R51006), General Projects National Fund (Project No. 32072291), National Key R & D Projects (Project No. 2020YFD0900901), National Key Research and Development Program of China (Project No. 2018YFC1602101), National Natural Science Foundation of China of China (Project No. 32001622), Guangdong Basic and Applied Research Foundation (Project No. 2021A1515011060), Fundamental and Applied Basic Research Fund for Young Scholars of Guangdong Province (Project No. 2019A1515110823), Science and Technology Commissioner Project of Guangzhou (Project No. GZKTP201937), Guangdong University Youth Innovation Talent Project (Project No. KA2001957), Key Generic Technology System of the Agricultural Industry in Guangdong Province (Project No. 2019KJ139), and Guangdong Key Laboratory of Science and Technology of Lingnan Specialty Food (Project No. 2021B1212040013).

## Data availability statement

The data that support the findings of this study are available from the corresponding author upon reasonable request.

## Institutional review board statement

The study was conducted in accordance with the Declaration of Helsinki, and the protocol was approved by the Ethics Committee through an animal production license issued by the Zhejiang Animal Ethics Committee (SYXK (Zhejiang) 2021–0025, Meat quality certificate of Food Co., Ltd.: 30000490535 approved for use).

## Ethical approval

Ethics approval was not required for this research.

## CRediT authorship contribution statement

**Tengfei Zhao:** Investigation, Methodology, Formal analysis, Data curation, Visualization, Writing – original draft. **Zhongqi Cao:** Investigation, Methodology. **Jin Yu:** Validation, Investigation, Resources, Supervision. **Xudong Weng:** Validation, Investigation, Resources, Supervision. **Sootawat Benjakul:** Validation, Writing – review & editing. **Alessandra Guidi:** Validation, Writing – review & editing. **Xiaoguo Ying:** Conceptualization, Project administration, Supervision, Writing – review & editing. **Lukai Ma:** Conceptualization, Project administration, Supervision, Writing – review & editing. **Gengsheng Xiao:** Supervision, Validation. **Shanggui Deng:** Validation, Writing – review & editing. All authors have read and agreed to the published

version of the manuscript.

## Declaration of competing interest

The authors declare that they have no known competing financial interests or personal relationships that could have appeared to influence the work reported in this paper.

## Acknowledgments

We would like to thank the Key Laboratory of Seafood Health Risk Factors of Zhejiang Ocean University for providing the scientific research platform.

## Appendix A. Supplementary data

Supplementary data to this article can be found online at <https://doi.org/10.1016/j.crfs.2022.04.012>.

## References

- Ade, C.J., Rosenkranz, S.K., Harms, C.A., 2014. The effects of short-term fish oil supplementation on pulmonary function and airway inflammation following a high-fat meal. *Eur. J. Appl. Physiol.* 114 (4), 675–682. <https://doi.org/10.1007/s00421-013-2792-7>.
- Ana, B., María, H.T., Iria, S., Ortega, M.J., Cristina, G.G., Marina, B.P., 2020. Types and distribution of bioactive polyunsaturated aldehydes in a gradient from mesotrophic to oligotrophic waters in the alborán sea (western mediterranean). *Mar. Drugs* 18 (3), 159–167. <https://doi.org/10.3390/md18030159>.
- Cao, J., Feng, A.G., He, Y.F., Wang, J.M., Liu, Z.Y., Xia, G.H., 2021. The effect and mechanism of four drying methods on the quality of tilapia fillet products. *Food Frontiers* 1–12. <https://doi.org/10.1002/fft2.124>.
- Chen, K., Li, E., Xu, C., Wang, X.D., Li, H.F., Qin, J.G., 2018. Growth and metabolomic responses of Pacific white shrimp (*Litopenaeus vannamei*) to different dietary fatty acid sources and salinity levels. *Aquaculture* 499, 329–340. <https://doi.org/10.1016/j.aquaculture.2018.09.056>.
- Chen, Q.S., Wang, X.C., Cong, P.X., Liu, Y.J., Wang, Y.M., Xu, J., 2017. Mechanism of phospholipid hydrolysis for oyster *Crassostrea plicatula* phospholipids during storage using shotgun lipidomics. *Lipids* 52 (12), 1045–1058. <https://doi.org/10.1007/s11745-017-4305-7>.
- Chen, X., Luo, J., Lou, A., Wang, Y., Yang, D.W., Shen, Q.W.W., 2021. Duck breast muscle proteins, free fatty acids and volatile compounds as affected by curing methods. *Food Chem.* 338, 128138–128148. <https://doi.org/10.1016/j.foodchem.2020.128138>.
- Chie, Y., Yukari, N., Hir, G., Makoto, S., Yu, H., Ken, T., 2021. Reduction of fatty liver in rats by nicotinamide via the regeneration of the methionine cycle and the inhibition of aldehyde oxidase. *J. Toxicol. Sci.* 46 (1), 31–42. <https://doi.org/10.2131/jts.46.31>.
- Chen, Y.P., Cai, D.D., Li, W.Q., Blank, I., Liu, Y., 2021. Application of gas chromatography-ion mobility spectrometry (GC-IMS) and ultrafast gas chromatography electronic-nose (uf-GC E-nose) to distinguish four Chinese freshwater fishes at both raw and cooked status. *J. Food Biochem.*, e13840 <https://doi.org/10.1111/jfbc.13840>.
- Crexli, V.T., Monte, M.L., Soares, L.A.D.S., Pinto, L.A.A., 2009. Production and refinement of oil from carp (*Cyprinus carpio*) viscera. *Food Chem.* 119 (3), 945–950. <https://doi.org/10.1016/j.foodchem.2009.07.050>.
- Cui, Z.K., Yan, H., Manoli, T., Mo, H.Z., Li, H.B., Zhang, H., 2020. Changes in the volatile components of squid (*Illex argentinus*) for different cooking methods via headspace–gas chromatography–ion mobility spectrometry. *Food Sci. Nutr.* 8 (10), 5748–5762. <https://doi.org/10.1002/fsn3.1877>.
- De, J.D., Taormina, E.I., Brien, D.J., 2017. Detection and characterization of volatile organic compounds from burned human and animal remains in fire debris. *Sci. Justice* 57 (2), 118–127. <https://doi.org/10.1016/j.scijus.2016.12.002>.
- Deng, S.Y., Liu, Y.H., Huang, F., Liu, J.Q., Han, D., Zhang, C.H., 2021. Evaluation of volatile flavor compounds in bacon made by different pig breeds during storage time. *Food Chem.* 357, 129765–129777. <https://doi.org/10.1016/j.foodchem.2021.129765>.
- Donovan, M.G., Selmin, O.I., Stillwater, B.J., Neumayer, L.A., Romagnolo, D.F., 2020. Do olive and fish oils of the mediterranean diet have a role in triple negative breast cancer prevention and therapy? An exploration of evidence in cells and animal models. *Front. Nutr.* 7, 571455–571463. <https://doi.org/10.3389/fnut.2020.571455>.
- Dou, P.P., Feng, X.C., Cheng, X.G., Guan, Q.H., Wang, J.L., Qian, S., 2021. Binding of aldehyde flavour compounds to beef myofibrillar proteins and the effect of nonenzymatic glycation with glucose and glucosamine. *Lebensm. Wiss. Technol.* 144, 111198–111208. <https://doi.org/10.1016/j.lwt.2021.111198>.
- Du, Q.W., Zhou, L.H., Li, M.H., Fei, L.U., Liu, J.H., Ding, Y.T., 2022. Omega-3 polyunsaturated fatty acid encapsulation system: physical and oxidative stability, and medical applications. *Food Frontiers* 1–17. <https://doi.org/10.1002/fft2.134>.

- Duan, Z.L., Dong, S.L., Dong, Y.W., Gao, Q.F., 2021a. Geographical origin identification of two salmonid species via flavor compound analysis using headspace-gas chromatography-ion mobility spectrometry combined with electronic nose and tongue. *Food Res. Inter.* 145, 110385–110395. <https://doi.org/10.1016/j.foodres.2021.110385>.
- Duan, Z.L., Dong, S.L., Sun, Y.X., Dong, Y.W., Gao, Q.F., 2021b. Response of Atlantic salmon (*Salmo salar*) flavor to environmental salinity while culturing between freshwater and seawater. *Aquaculture* 530. <https://doi.org/10.1016/j.aquaculture.2020.735953>.
- Elavarasan, K., Shamasundar, B.A., 2021. Antioxidant properties of papain mediated protein hydrolysates from fresh water carps (*Catla catla*, *Labeo rohita* and *Cirrhinus mrigala*) and its application on inhibition of lipid oxidation in oil sardine mince during ice storage. *J. Food Sci. Technol.* 1–10. <https://doi.org/10.1007/s13197-021-05053-0>.
- Emre, Y., 2021. Determination of fish quality parameters with low cost electronic nose. *Food Biol.* 41. <https://doi.org/10.1016/j.foodbi.2021.100948>.
- Encina, C., Ruiz, G.M., Holgado, F., Giménez, B., Vergara, C., Robert, P., 2018. Effect of spray-drying with organic solvents on the encapsulation, release and stability of fish oil. *Food Chem.* 263, 283–291. <https://doi.org/10.1016/j.foodchem.2018.05.026>.
- Galindo, A., Garrido, D., Monroig, Ó., Pérez, J.A., Betancor, M.B., Acosta, N.G., 2021. Polyunsaturated fatty acid metabolism in three fish species with different trophic level. *Aquaculture* 530. <https://doi.org/10.1016/j.aquaculture.2020.735761>.
- Granato, D., Santos, J.S., Escher, G.B., Ferreira, B.L., Maggio, R.M., 2018. Use of principal component analysis (PCA) and hierarchical cluster analysis (HCA) for multivariate association between bioactive compounds and functional properties in foods: a critical perspective. *Trends Food Sci. Technol.* 72, 83–90. <https://doi.org/10.1016/j.tifs.2017.12.006>.
- IlesanmiOyelere, B.L., Coad, J., Roy, N.C., Kruger, M.C., 2020. Dietary patterns, body composition, and bone health in New Zealand postmenopausal women. *Front. Nutr.* 7, 563689–563699. <https://doi.org/10.3389/fnut.2020.563689>.
- Jadwiga, H., Magdalena, G., Agnieszka, S., Joanna, F., 2019. Weight loss program is associated with decrease  $\alpha$ -tocopherol status in obese adults. *Clin. Nutr.* 38 (4), 1861–1870. <https://doi.org/10.1016/j.clnu.2018.07.011>.
- Jia, S.L., Li, Y., Zhuang, S.A., Sun, X.H., Zhang, L.T., Shi, J., 2021. Biochemical changes induced by dominant bacteria in chill-stored silver carp (*Hypophthalmichthys molitrix*) and GC-IMS identification of volatile organic compounds. *Food Microbiol.* 84, 103248–103259. <https://doi.org/10.1016/j.fm.2019.103248>.
- Jia, Z.X., Shi, C., Wang, Y.B., Yang, X.T., Zhang, J.R., Ji, Z.T., 2020. Nondestructive determination of salmon fillet freshness during storage at different temperatures by electronic nose system combined with radial basis function neural networks. *Int. J. Food Sci. Technol.* 55 (5), 2080–2091. <https://doi.org/10.1111/ijfs.14451>.
- Kazuo, M., Mariko, U., Masashi, H., 2018. Effective prevention of oxidative deterioration of fish oil: focus on flavor deterioration. *Annu. Rev. Food Sci. Technol.* 9 (1), 209–226. <https://doi.org/10.1146/annurev-food-030117-012320>.
- Li, H., Tang, X.Y., Wu, C.J., Yu, S.J., 2021. Maillard reaction in Chinese household-prepared stewed pork balls with brown sauce: potentially risky and volatile products. *Food Sci. Hum. Wellness* 10 (2), 221–230. <https://doi.org/10.1016/j.fshw.2021.02.012>.
- Li, M., Lin, S.Y., Wang, R.C., Gao, D., Bao, Z.J., Chen, D., 2022. Inhibitory effect and mechanism of various fruit extracts on the formation of heterocyclic aromatic amines and flavor changes in roast large yellow croaker (*Pseudosciaena crocea*). *Food Control* 131, 108410–108420. <https://doi.org/10.1016/j.foodcont.2021.108410>.
- Li, L., Wang, C.C., Jiang, S., Li, R., Zhang, T.T., Xue, C.H., 2020. The absorption kinetics of Antarctic krill oil phospholipid liposome in blood and the digestive tract of healthy mice by single gavage. *Food Sci. Hum. Wellness* 9 (1), 88–94. <https://doi.org/10.1016/j.fshw.2020.01.002>.
- Li, X.X., Wang, K., Yang, R.W., Dong, Y.F., Lin, S.Y., 2020. Mechanism of aroma compounds changes from sea cucumber peptide powders (SCPPs) under different storage conditions. *Food Res. Inter.* 128, 108757–108767. <https://doi.org/10.1016/j.foodres.2019.108757>.
- Lysfjord, S.S., Ateshm, G., Gong, Y.Y., Dalia, D., Ghana, V., Mette, S., 2021. Growth, chemical composition, histology and antioxidant genes of atlantic salmon (*Salmo salar*) fed whole or pre-processed nannochloropsis oceanica and tetraselmis sp. *Fishes* 6 (3), 23–33. <https://doi.org/10.3390/fishes6030023>.
- Ma, L.K., Liu, G.Q., Cheng, W.W., Liu, X.Q., Brennan, C., Brennan, M.A., 2021. The effect of heating on the formation of 4-hydroxy-2-hexenal and 4-hydroxy-2-nonenal in unsaturated vegetable oils: evaluation of oxidation indicators. *Food Chem.* 321, 126603–126611. <https://doi.org/10.1016/j.foodchem.2020.126603>.
- Ma, L.K., Liu, G.Q., Cheng, W.W., Liu, X.Q., Liu, H.F., Wang, Q., 2020. Formation of malondialdehyde, 4-hydroxy-hexenal and 4-hydroxy-nonenal during deep-frying of potato sticks and chicken breast meat in vegetable oils. *Int. J. Food Sci.* 55 (4), 1833–1842. <https://doi.org/10.1111/ijfs.14462>.
- Malik, I.A., Elgasim, E.A., Adiamo, O.Q., Ali, A.A., Mohamed, A.I.A., 2021. Effect of frozen storage on the biochemical composition of five commercial freshwater fish species from River Nile, Sudan. *Food Sci. Nutr.* 9 (7), 3758–3767. <https://doi.org/10.1002/fsn3.2340>.
- Mi, R.F., Chen, X., Xiong, S.Y., Qi, B., Li, J.P., Qiao, X.L., 2021. Predominant yeasts in Chinese Dong fermented pork (Nanx Wudl) and their aroma-producing properties in fermented sausage condition. *Food Sci. Hum. Wellness* 10 (2), 231–240. <https://doi.org/10.1016/j.fshw.2021.02.013>.
- Mutlu, I.A., Catalkaya, G., Capanoglu, E., Karbancioglu, G.F., 2021. Antioxidant and antimicrobial activities of fennel, ginger, oregano and thyme essential oils. *Food Frontiers* 2 (4), 508–518. <https://doi.org/10.1002/fft2.77>.
- Navarro, H.M.D., Varela, L.A., Romero, M.J.M., Piquer, M.C., Bullón, P., Forbes, H.T.Y., José, L., Quiles, J.L., 2020. Twenty-four months feeding on unsaturated dietary fats (virgin olive, sunflower, or fish oil) differentially modulate gingival mitochondria in the rat. *eFood* 1 (1), 61–68. <https://doi.org/10.2991/efood.k.190802.002>.
- Salsinha, A.S., Rodríguez, A.L.M., Relvas, J.B., Pintado, M.E., 2021. Fatty acids role on obesity induced hypothalamus inflammation: from problem to solution—A review. *Trends Food Sci. Technol.* 112, 592–607. <https://doi.org/10.1016/j.tifs.2021.03.042>.
- Song, G.S., Dai, Z.Y., Shen, Q., Peng, X., Zhang, M.N., 2018. Analysis of the changes in volatile compound and fatty acid profiles of fish oil in chemical refining process. *Eur. J. Lipid Sci. Technol.* 120 (2). <https://doi.org/10.1002/ejlt.201700219>.
- Sullivan, J.C., Budge, S.M., 2012. Fish oil sensory properties can be predicted using key oxidative volatiles. *Eur. J. Lipid Sci. Technol.* 114 (5), 496–503. <https://doi.org/10.1002/ejlt.201100330>.
- Thimmappa, M.N., Reddy, A.M., Prabhu, R.M., Elavarasan, K., 2019. Quality changes in deep-sea shrimp (*aristotelecoi*) during ice storage: biochemical and organoleptic changes. *Agric. Res. (Wash. D C)* 8 (4), 497–504. <https://doi.org/10.1007/s40003-019-00397-8>.
- Tian, X., Li, Z.J., Chao, Y.Z., Wu, Z.Q., Zhou, M.X., Xiao, S.T., 2020. Evaluation by electronic tongue and headspace-GC-IMS analyses of the flavor compounds in dry-cured pork with different salt content. *Food Res. Inter.* 137, 109456–109466. <https://doi.org/10.1016/j.foodres.2020.109456>.
- Tu, C.H., Qi, X.E., Shui, S.S., Lin, H.M., Soottawat, B., Zhang, B., 2021. Investigation of the changes in lipid profiles induced by hydroxyl radicals in whiteleg shrimp (*Litopenaeus vannamei*) muscle using LC/MS-based lipidomics analysis. *Food Chem.* 369, 130925–130935. <https://doi.org/10.1016/j.foodchem.2021.130925>.
- Valdés, A., Beltrán, A., Mellinas, C., Jiménez, A., Garrigós, M.C., 2018. Analytical methods combined with multivariate analysis for authentication of animal and vegetable food products with high fat content. *Trends Food Sci. Technol.* 77, 120–130. <https://doi.org/10.1016/j.tifs.2018.05.014>.
- Wang, S.Q., Chen, H.T., Sun, B.G., 2020. Recent progress in food flavor analysis using gas chromatography–ion mobility spectrometry (GC–IMS). *Food Chem.* 315. <https://doi.org/10.1016/j.foodchem.2019.126158>.
- Yang, Y., Wang, B., Fu, Y., Shi, Y.G., Chen, F.L., Guan, H.N., 2021. HS-GC-IMS with PCA to analyze volatile flavor compounds across different production stages of fermented soybean whey tofu. *Food Chem.* 346. <https://doi.org/10.1016/j.foodchem.2020.128880>.
- Yao, W.S., Cai, Y.X., Liu, D.Y., Zhao, Z.N., Zhang, Z.H., Ma, S.Y., 2020. Comparative analysis of characteristic volatile compounds in Chinese traditional smoked chicken (specialty poultry products) from different regions by headspace–gas chromatography–ion mobility spectrometry. *Poultry Sci.* 99 (12), 7192–7201. <https://doi.org/10.1016/j.psj.2020.09.011>.
- Yu, L.J., Wang, Y., Wen, H., Jiang, M., Wu, F., Tian, J., 2021. Synthesis and evaluation of acetylferulic paeonol ester and ferulic paeonol ester as potential antioxidants to inhibit fish oil oxidation. *Food Chem.* 365, 130384–130394. <https://doi.org/10.1016/j.foodchem.2021.130384>.
- Zhang, B., Yan, H.B., Su, L.J., Chen, X.N., 2020. Kappa-carrageenan oligosaccharides retard the progression of protein and lipid oxidation in mackerel (*Scomber japonicus*) fillets during frozen storage. *RSC Adv.* 10 (35), 20827–20836. <https://doi.org/10.1039/d0ra03431b>.
- Zhang, D.G., Zhao, T., Christer, H., Ye, H.M., Xu, X.J., Luo, Z., 2021. Oxidized fish oils increased lipid deposition via oxidative stress-mediated mitochondrial dysfunction and the CREB1-Bcl2-Beclin1 pathway in the liver tissues and hepatocytes of yellow catfish. *Food Chem.* 360, 129814–129825. <https://doi.org/10.1016/j.foodchem.2021.129814>.
- Zhang, Q., Ding, Y.C., Gu, S.Q., Zhu, S.C., Zhou, X.X., Ding, Y.T., 2020. Identification of changes in volatile compounds in dry-cured fish during storage using HS-GC-IMS. *Food Res. Inter.* 137, 109339–109349. <https://doi.org/10.1016/j.foodres.2020.109339>.
- Zhao, T.F., Bulei, S., Ying, X.G., Chiara, S., Soottawat, B., Ma, L.K., 2021a. Role of lipid deterioration on the quality of aquatic products during low-temperature storage: a lipidomics-based study using large yellow croaker (*Larimichthys crocea*). *Int. J. Food Sci. Technol.* 57, 1026–1039. <https://doi.org/10.1111/ijfs.15465>.
- Zhao, T.F., Soottawat, B., Chiara, S., Ying, X.G., Ma, L.K., Xiao, G.S., 2021b. Changes of volatile flavor compounds in large yellow croaker (*Larimichthys crocea*) during storage, as evaluated by headspace gas chromatography–ion mobility spectrometry and principal component analysis. *Foods* 10 (12), 1–15. <https://doi.org/10.3390/foods10122917>.
- Zhou, H.M., Zhao, B., Zhang, S.L., Wu, Q.R., Zhu, N., Li, S., 2021. Development of volatiles and odor-active compounds in Chinese dry sausage at different stages of process and storage. *Food Sci. Hum. Wellness* 10 (3), 316–326. <https://doi.org/10.1016/j.fshw.2021.02.023>.